Fast oxidation processes from emission to ambient air introduction of aerosol emitted by residential log wood stoves

Nalin Federica, B. Golly, Pelletier Charles, Aujay-Plouzeau Robin, Verlhac Stéphane, Dermigny Adrien, Fievet Amandine, Karoski Nicolas, Dubois Pascal, Collet Serge, et al.

Fast oxidation processes from emission to ambient air introduction of aerosol emitted by residential log wood stoves

*Federica Nalin[1], Benjamin Golly[2], Jean-Luc Besombes[2], Charles Pelletier[2], Robin Aujay-Plouzeau[1], Stéphane Verlhac[1], Adrien Dermigny[1], Amandine Fievet[1], Nicolas Karoski[1], Pascal Dubois[1], Serge. Collet[1], Olivier Favez[1] and Alexandre Albinet[1,]**

[1]Institut National de l'Environnement industriel et des RISques (INERIS), 60550 Verneuil en Halatte, France

[2]Université Savoie Mont-Blanc, LCME, F-73000 Chambéry, France.

Keywords

Biomass burning; Emission factors; PAH; Nitro-PAH; Oxy-PAH; gas/particle partitioning

Corresponding Author

* alexandre.albinet@ineris.fr; alexandre.albinet@gmail.com

Abstract

Little is known about the impact of post-combustion processes, condensation and dilution, on the aerosol concentration and chemical composition from residential wood combustion. The evolution of aerosol emitted by two different residential log wood stoves (old and modern technologies) from emission until it is introduced into ambient air was studied under controlled "real" conditions. The first objective of this research was to evaluate the emission factors (EF) of polycyclic aromatic hydrocarbons (PAH) and their nitrated and oxygenated derivatives from wood combustion. These toxic substances are poorly documented in the literature. A second objective was to evaluate the oxidation state of the wood combustion effluent by studying these primary/secondary compounds. EFs of Σ_{37}PAHs and Σ_{27}Oxy-PAHs were in the same range and similar to those reported in literature (4-240 mg kg^{-1}). Σ_{31}Nitro-PAH EFs were 2 to 4 orders of magnitude lower (3.10^{-2}-8.10^{-2} mg kg^{-1}) due to the low temperature and low emission of NO_2 from wood combustion processes. An increase of equivalent EF of PAH derivatives was observed suggesting that the oxidation state of the wood combustion effluent from the emission point until its introduction in ambient air changed in a few seconds. These results were confirmed by the study of both, typical compounds of SOA formation from PAH oxidation and, PAH ratio-ratio plots commonly used for source evaluation.

1. Introduction

During this last decade in Europe, the use of wood burning for residential heating has significantly increased because it is a renewable source of energy. As a result, it is becoming a significant source of particulate matter (PM) in ambient air. Wood combustion could contribute to about 30-60% of the carbonaceous fraction of PM and, in the winter season, to about 50% of the total level of $PM_{2.5}$ even in large cities such as Paris or London (Denier van der Gon et al., 2015, Favez et al., 2009, Favez et al., 2010, Herich et al., 2014, Maenhaut et al., 2012, Viana et al., 2016). In France, emission inventories estimate that residential heating, and in particular wood combustion, accounts for about 31% of the total $PM_{2.5}$ emissions (CITEPA, 2015).

Emissions of PM from woodstoves used for residential heating are difficult to evaluate due to their strong semi-volatile nature and to the fast physicochemical transformation once they are injected into the atmosphere. Semi-volatile compounds (mainly organic species) remain in the gaseous phase in the chimney and are not taken into account using PM reference measurement methods (Nussbaumer et al., 2008). Once in the atmosphere, they can remain in the gas phase, condense on pre-existing particles or form new particles by nucleation and/or photo-oxidation processes. A significant difference could be observed between the emission levels of PM, measured using reference methods that take into account only the solid PM fraction, and the concentration levels actually measured in ambient air and/or in the field close of the emission sources. The difference could reach a factor of 2 to 3 when PM concentration levels in ambient air are normalized to the same O_2 concentration found in emission measurements (Nussbaumer et al., 2008, Viana et al., 2016). To date, these processes are not well understood and not included in atmospheric chemical/transport models used to forecast air quality. It follows then, that modelled PM concentrations and the contribution of wood combustion to ambient air PM

concentrations and PM emission inventories are nowadays underestimated (Denier van der Gon et al., 2015). To better assess the impact of the combustion of wood used for residential heating on the PM concentration levels, a better description and understanding of the physicochemical properties of the emissions and of their formation/transformation processes in the field close to the source are needed.

The impact of PM on ambient air quality and health is strongly associated to its chemical composition and content of toxic species. PAHs have been largely studied and regulated in ambient air (European Official Journal, 2004), due to their recognized carcinogenic and mutagenic properties (IARC, 2010). In contrast, PAH derivatives including nitrated and oxygenated PAHs (NPAHs and OPAHs, respectively) were given less attention although they are probably more toxic than their parent compounds (Durant et al., 1996, Durant et al., 1998, IARC, 2012, Pedersen et al., 2004, Pedersen et al., 2005). Interestingly, some PAH derivatives are now classified as probably or possibly carcinogenic to humans (groups 2A and 2B, respectively) (IARC, 2013).

NPAHs and OPAHs are introduced in the atmosphere, as a result of direct emission during combustion (including biomass burning) (Environmental Health Criteria (EHC) 229, 2003, Rogge et al., 1993, 1998, Schauer et al., 1999, 2001, 2002, Zielinska et al., 2004) and by secondary formation through homogeneous (in the gas phase) or heterogeneous gas/particle photooxidation processes (Arey et al., 1986, Keyte et al., 2013). The latter involve the parent PAHs that undergo reaction with atmospheric oxidants such as NO_2, O_3, OH and NO_3. PAH derivatives are also of scientific interest because they are typically found in secondary organic aerosol (SOA) formed via the photooxidation of PAHs. In fact, recent studies show that PAHs could be a significant source of SOA in urban locations (Chan et al., 2009, Chen et al., 2016,

Kautzman et al., 2010, Pye and Seinfeld, 2010, Shakya and Griffin, 2010, Zhang and Ying, 2011).

The main objective of the Champrobois research project was to study the evolution of aerosol emitted by residential log wood stoves (RWS) from emission to their introduction in the ambient air under controlled real conditions. Here, the specific objectives were first, to evaluate the emission factors (EFs) of PAH and PAH derivatives from combustion of wood, poorly documented in the literature (Bruns et al., 2015, Environmental Health Criteria (EHC) 229, 2003, Fine et al., 2001, 2002, Fine et al., 2004a, 2004b, Gonçalves et al., 2010, Gullett et al., 2003, Iinuma et al., 2007, Orasche et al., 2012, Orasche et al., 2013, Rogge et al., 1998, Schauer et al., 2001, Shen et al., 2012a, Shen et al., 2012b, Vicente et al., 2015), and second, to evaluate the oxidation state of the effluent from wood combustion studying these primary/secondary compounds.

2. Material and methods

1.1. Wood burning experiments

Wood combustion experiments were carried out in the INERIS' fire gallery in March 2013 (Figure S1 in the Supplementary Material, SM). The fire gallery (of about 3×3.5×50 m) has a controlled ventilation system that allows the extraction of the combustion gases. The system includes several air flow measuring points (Mac Caffrey probes) and the dilution factor can be easily adjusted and determined. RWS were placed in the bottom vertical part of the fire gallery. This large pipe (3×2 m), permitting a minimization of the wall effects, was instrumented in its upward and downward parts for the measurement of the different physical and chemical parameters.

Experiments were performed using two kinds of RWS (old and modern technology = 4* and 5*, respectively) (Table S1). The 4* RWS was a cast-iron stove with only one air inlet, while the 5* RWS is made of steel with bricks inside and includes several air inlets (primary and secondary).

The RWS were connected to an insulated duct (CEN (European Comittee for Standardization), 2013), except for its height (≈4 m) and used as an exhaust pipe. RWS smoke exhausts were maintained at a temperature >150 °C in order to avoid any physicochemical transformation processes of the semi-volatile compounds before their introduction in the vertical part of the fire gallery. The air flow in the gallery (constant flow from 10×10^3 to 24×10^3 $Nm^3\ h^{-1}$, depending on the experiment) and exhaust pipe length were adjusted in order to obtain the required dilution factors in the different sampling locations (Table 1, Figure S1). The determination of the dilution factors in each sampling point is detailed below.

Wood burning experiments were performed in two different conditions: nominal and reduced outputs (Table 1). Duplicates were performed in nominal output condition while single experiments were performed in reduced output condition. One single type of wood, beech (typically used in France) from the same wood batch (moisture=12%), was used for all experiments.

The fire in the RWS was started using a small quantity of wood and then preheated systematically before each test with a first wood load. Combustion experiments were carried out with weighed wood loads, in agreement with the device power, the test duration (around 1 hour), and in order to reach a minimum temperature in the exhaust pipe (>150 °C). For reduced output tests, the amount of wood put into the stove was lower to minimize the experiment durations. Loads were put in the wood stove once the preload was fully burned (i.e. no remaining material

to burn in the fireplace and CO_2 exhaust concentration below 4%). Note that the loads used in the different experiments were more representative of a common use of the wood stoves than of the use during standard evaluations.

1.2. Sampling locations and pollutants

Samplings and measurements were performed at four different locations (Figure S1): emission source (E), at about 0.5 m from the chimney exhaust (named very close field, VCF, dilution factor of about 10-20), at 20 m from the emission exhaust (named close field, CF, dilution factor of about 500) and at the entrance of the fire gallery (named ambient air, AA) in order to evaluate and subtract the ambient air contribution to the pollutant emission concentrations. Manual measurements and samplings began immediately after the wood load addition in the RWS and ended when the initial test conditions were reached.

Several parameters, such as smoke temperature, air flow, O_2, NO_x, CO, CO_2, total VOCs concentrations, were monitored continuously by using automatic sensors or analysers (E, VCF, CF) (Tables S2 to S5). “On-line” physicochemical characterization of the wood combustion smoke was performed using TEOM-50, TEOM-FDMS (Thermo), FIDAS 200s (Palas) for PM mass determination (solid and solid + condensable fractions) (VCF, CF and AA, respectively).

Manual samplings (“off-line”) (gaseous and particulate phases) were carried out at the different sampling locations for studying several parameters and pollutants including humidity (E, VCF), PM (solid and condensable fractions) (E, VCF), PM chemical composition including the analysis of PAHs and their nitrated and oxygenated derivatives (NPAHs and OPAHs) (for all, AA, E, VCF, CF). All the PM “on-line” and “off-line” measurements and samplings were performed on the $PM_{2.5}$ fraction ($D_p < 2.5$ µm).

An overview of the main parameters (gaseous pollutants and PM mass) observed during the different wood burning experiments is shown in Table S6.

1.3. PAH, OPAH and NPAH samplings

At the emission source location, samplings of PAHs, OPAHs and NPAHs were performed using two parallel sampling trains with different sampling flows (10 L min^{-1}, isokinetic conditions, and 2 L min^{-1}). Sampling probe and filter temperatures were regulated at about 125 °C. Particulate and gaseous phase were collected on quartz fibre filters (Whatman, QM-A, Ø=75 mm) and on Amberlite XAD-2 resin (80 g, Aldrich), respectively.

At the VCF the same kind of instrumentation was carried out for the study of these toxic compounds with a sampling flow of 10 L min^{-1} (subdivision of a common sampling train at 30 L min^{-1}, isokinetic conditions) and a temperature regulation (probe and filter at about 50 °C) (M1). In parallel, samplings were performed using a low volume sampler (Partisol, Model 2000, R&P) at 10 L min^{-1} on tissuquartz filter (Pallflex, Ø=47 mm) and PUFs (polyurethane foams, Tisch Environmental, 75 mm length) for particulate and gaseous phases, respectively. The sampling train was not heated but only insulated (M2).

In the CF and AA, samplings were performed using a high-volume sampler (DA-80, Digitel, 30 m^3 h^{-1}, $PM_{2.5}$ sampling head) on tissuquartz filter (Pallflex, Ø=150 mm) and PUFs (polyurethane foams, Tisch Environmental, 79 mm length).

Before sampling, filters were heated for 12 hours at 500 °C to remove any organic contaminants. XAD-2 and PUFs were pre-washed with dichloromethane or hexane/acetone (sequentially) using pressurized liquid extraction (PLE, Dionex, ASE 350) (Zielinska, 2008). E

and VCF sampling probes and glassware (bubblers) were pre-washed using deionized water and organic solvents (acetone, dichloromethane) before use.

Overall, about 100 samples were collected and analyzed for their PAHs and PAH derivatives content, including field blanks and fire gallery blanks. After collection, all samples were wrapped in aluminum foil, sealed in polyethylene bags, and stored at -10 °C until analysis.

1.4. PAHs, OPAHs and NPAH sample extraction and analysis

PUF and XAD-2 samples were extracted with acetone and dichloromethane, respectively, using PLE (Dionex, ASE 200 or 350, depending on the sample size). The following conditions were adopted: 80 °C, 100 bars, 2 cycles and static time of 15 minutes. For PUFs, acetone was chosen to avoid any sampling media degradation. All extracts were then divided into two equal fractions by weighting (balance precision = 0.1 g) for the analysis of PAHs (LCME) and of NPAHs and OPAHs (INERIS), respectively.

E and VCF filter samples, collected using emission-like sampling trains, were divided in two equal parts by weighting (balance precision=0.1 mg). Analyses of VCF Partisol and AA, CF particulate samples were performed on filter punches of 1 cm^2 and 47 mm diameter, respectively. Filter sections/punches were then used for the analysis of PAHs and PAH derivatives (LCME and INERIS, respectively).

Briefly, for PAH quantification, filter sections/punches (AA, E, VCF and CF) were extracted by PLE [Dionex, ASE 200; 100 °C, 100 bars, 2 cycles with methanol/dichloromethane (10/90, v/v) and acetone/ dichloromethane (50/50, v/v), 5 min]. Extracts were reduced under a nitrogen stream (Zymark, Tubovap II) close to dryness and dissolved in a known volume of ACN or DCM before analysis. For NPAHs and OPAHs, particulate samples (AA, E, VCF and CF) were

extracted using the QuEChERS-like extraction procedure (Quick Easy Effective Rugged and Safe) (Albinet et al., 2013, Albinet et al., 2014).

For both PLE and QuEChERS procedures, the samples (filter punches, PUFs or XAD-2 resins) were spiked with known amounts of deuterated NPAH and OPAH surrogate standards before extraction (addition of 5 µL, 25 µL or 50 µL, depending on the sample, of a surrogate mixed standard solution of five deuterated NPAHs and two deuterated OPAHs, at approximately 1 ng μL^{-1} in ACN) (Albinet et al., 2014).

For both gaseous and particulate samples, 37 PAHs (Table 2) were quantified by HPLC-Fluorescence (Perkin-Elmer, LC240; column EC 250/4.6 Nucleodur C18 PAH, 3 µm) (18 PAHs quantified) (Besombes et al., 2001, Goriaux et al., 2006) and by GC/MS (HP 6890 and 5973; Column Optima 5 Accent, 30 m×0,25 mm×0,25 µm, Macherey Nagel) (19 methyl-PAHs quantified) (Golly et al., 2015). Before injection in GC/MS, extracts were spiked with 50 ng of Benzo[a]Anthracene-d_{12} as labelled internal standard. Finally, 27 OPAHs and 31 NPAHs were quantified by GC-NICI/MS (Albinet et al., 2006, Albinet et al., 2014) (Tables 3 and 4). Before analysis, purified samples were spiked with known amounts of two labeled internal standards (1-nitropyrene-d_9 and 9-fluorenone-d_8; 5, 25 or 50 ng added, depending on the sample) to evaluate the recoveries of labeled NPAH and OPAH surrogates.

1.5. Quality assurance/Quality control

Before each wood burning experiment, fire gallery blanks were systematically performed. Concentration levels of pollutants continuously monitored in VCF and CF were compared to the ones observed during combustion experiments. Gaseous and particulate phase samplings, for about 1-2 hours, were performed in CF and AA in order to evaluate the level of contamination of

carbonaceous species including PAHs and PAH derivatives. Results show that for $PM_{2.5}$, fire blank gallery concentration levels accounted for less than 1% of the $PM_{2.5}$ concentration levels observed during the wood burning combustion experiments. NO_x concentrations were 2-8 times lower than those measured at CF during combustion experiments and CO_2 concentrations were at about 420 ppm ($[CO_2]$>500 ppm during combustion experiments).

The levels of nitrated and oxygenated PAH derivatives on filters and PUFs were also evaluated in CF, to assess any possible contamination. For all individual PAHs, NPAHs and OPAHs, fire gallery blank concentration levels accounted for less than 10%, and generally for less than 1%, of the concentration levels observed during wood combustion experiments. Most of the NPAHs were not detected in fire gallery blanks.

All these results demonstrated that no significant contamination due to previous combustion experiments occurred.

The equivalence of the two sampling trains used for samplings at the emission was checked for PM mass. No significant differences between the two sampling trains were observed showing and confirming that isokinetic sampling conditions are not fundamental for the emission-point study of PM emitted by RWS (Fraboulet, 2012).

Quality control for the quantification of PAHs and PAH derivatives was achieved by the analysis of standard reference materials (NIST SRM 1649b, urban dust and/or SRM 2787, PM_{10}). Results obtained were satisfactory and in good agreement with the certified, reference and indicative values and with the ones previously reported in the literature (Albinet et al., 2013, Albinet et al., 2014). Additionally, for PAHs, LCME participates every two years in national and European PAH analytical inter-comparison exercises. The last exercise showed results in good agreement with reference values (Verlhac and Albinet, 2015).

For NPAHs and OPAHs, a specific study of the calibration variability between the analytical sequences was performed (combination of two daily eight-point calibrations). Compounds with deviation larger than 30% were rejected and not considered in this study. This concerned phthalic anhydride, 1,2-naphthoquinone, 1,2-naphthalic anhydride, 2,3-naphthalenedicarboxylic anhydride, 5,6-chrysenequinone and 9-methyl-10-nitroanthracene. Finally, 31 NPAHs and 27 OPAHs were effectively quantified and their results are discussed in this paper.

2. Calculations

Dilution factors were determined using air flow or gaseous compounds (CO, CO_2, NO_x) concentration ratios measured at each sampling point. An example of the calculation of the dilution factor in VCF is given below:

$$\frac{[CO_2]_E - [CO_2]_{AA}}{[CO_2]_{VCF} - [CO_2]_{AA}} \qquad \text{Equation (1)}$$

PAH, NPAH and OPAH emission factors (EF) were calculated using the following equation:

$$EF_{PAHs,OPAHs,NPAHs} = \frac{[PAHs,OPAHs,NPAHs] \times DF \times WSEFl \times CD}{Mass\ of\ wood\ burned} \times 10^{-6} \qquad \text{Equation (2)}$$

With:

$EF_{PAHs,\ OPAHs,\ NPAHs}$ in mg kg^{-1} (dry mass basis).

[PAHs], [OPAHs], [NPAHs] in ng Nm^{-3} (gaseous + particulate phases), corrected for ambient air (AA) concentrations.

DF: dilution factor at the corresponding sampling point (Table 1).

CD: combustion duration (in hours) (Table 1).

WSEFl: wood stove emission flow in Nm^{-3} h^{-1} (for dry gas) (Table 1).

Mass of wood burned in kg (corrected for moisture content=12%) (Table 1).

3. Results and discussion

3.1. Emission factors (EFs) of PAHs, OPAHs and NPAHs

The EFs of the individual PAHs, OPAHs and NPAHs (gaseous + particulate phases), determined using the measurements performed at the emission, are presented in Tables 2 to 4. Individual EFs of PAHs, NPAHs and OPAHs in VCF and CF are available in Tables S7 to S12.

Overall, PAH and OPAH EFs were in the same range (EF Σ_{37} PAHs=28–240 and EF Σ_{27} OPAHs=4–33 mg kg^{-1}), while NPAH EFs were 2 to 4 orders of magnitude lower (EF Σ_{31} NPAHs=3.1×10^{-2}–7.5×10^{-2} mg kg^{-1}). By comparison to diesel engines, the low wood nitrogen content (<1%) together with the relatively low temperature and the low NO_2 emission from wood combustion processes induce a limited formation of nitrated species, including NPAHs (Scheepers and Bos, 1992, Shen et al., 2012a). Since OPAHs are probably more toxic than PAHs, these results suggest that evaluation of the OPAH EFs of RWS should be addressed in addition to those of PAHs.

EFs for individual compounds determined in this work were comparable with those reported in the literature for RWS or fire place emissions. For example, for PAHs, EFs varied from 6×10^{-2} to 4×10^{3} mg kg^{-1} and for OPAHs, from 1×10^{-2} to 3 mg kg^{-1} (Bruns et al., 2015, Fine et al., 2001, 2002, Fine et al., 2004a, 2004b, Gonçalves et al., 2010, Gullett et al., 2003, Iinuma et al., 2007, Orasche et al., 2012, Orasche et al., 2013, Rogge et al., 1998, Schauer et al., 2001, Shen et al., 2012a, Shen et al., 2012b, Vicente et al., 2015). Individual EFs of NPAHs are in agreement with

those reported in the only two studies available in the literature about the emission of NPAHs from residential wood burning (1.5×10^{-4}–7×10^{-3} mg kg^{-1}) (Shen et al., 2012a, Vicente et al., 2015).

As reported in previous studies, the dominant PAHs were naphthalene (34-55%), phenanthrene (10-25%), fluoranthene (3-10%) and pyrene (3-10%) (Gonçalves et al., 2010, Shen et al., 2012a). 1-Naphthaldehyde (60% and 15-40% in nominal and reduced output conditions, respectively), 1-acenaphthenone (15-20%), 9-fluorenone (8-25%), benzanthrone (3-30%), 1,4-naphthoquinone (2-10%) and 9,10-anthraquinone (2%) were the most abundant OPAHs. These results are in agreement with previous studies except for 1-H-phenalen-1-one reported as a major OPAH emitted by residential wood combustion but not analyzed in this work (Bruns et al., 2015, Fine et al., 2004a, 2004b, Gullett et al., 2003, Rogge et al., 1998). 1,8-Naphthalic anhydride was also reported as a major OPAH emitted by residential wood combustion (results focused only on the particulate phase) (Bruns et al., 2015, Gullett et al., 2003, Orasche et al., 2012, Orasche et al., 2013, Vicente et al., 2015). In this study, for the particulate phase, it was also the case with mainly benzo[b]fluorenone, benzanthrone, benz[a]antracene-7,12-dione and acenaphthenequinone. 1-Nitronaphthalene (8-20%), 2-nitronaphthalene (8-20%) and in specific experiments, 6-nitrobenzo[a]pyrene (7% in nominal output conditions), 3-nitrobiphenyl (reduced output) 9-nitroanthracene (20%, 5* RWS reduced output) and 1,8-dinitropyrene (4* RWS reduced output and 5* RWS nominal output) were the main NPAHs emitted by wood burning combustion. Both dominant NPAHs, namely 1- and 2-nitronaphthalene, were reported by previous authors (Shen et al., 2012a).

Finally, the results obtained showed that, for 5* RWS, the EFs of PAHs, OPAHs and, to a lesser extent, NPAHs were 2 to 5 times larger than those observed for the 4* RWS. Similar

results were also observed for the other pollutants studied, including PM (Table 1) and total VOCs (Table S6). All these results are in contradiction with the 5* RWS manufacturer's specifications. The new RWS technology, with secondary air inlet, should in theory improve the combustion. However, in our experimental conditions, that were more similar to a common use (notably in terms of RWS wood loading), the benefit with the tested 5* RWS was not observed. Normative tests of the RWS are probably done only in almost ideal conditions which are not representative of a common use.

3.2. Physicochemical evolution of the wood combustion effluent from E until CF

3.2.1. Gas/particle partitioning

Figure 1 shows the results obtained with the 5* RWS in nominal output conditions of the gas/particle partitioning (particulate fraction in %) of individual PAHs, NPAHs and OPAHs according to their molecular weight. Results for the other conditions and RWS are presented in Figures S1 to S6 (Annexes). In VCF, only the results from the emission-like sampling train are reported (heated sampling train) (M1). Results from the Partisol measurements (M2) were not taken into account. Since this sampling line was only thermally insulated, SVOC condensation processes were artificially increased and resulted probably in a bad evaluation of the gas/particle partitioning.

The results obtained show that the gas/particle partitioning of PAHs and PAH derivatives is quite linked to their molecular weight and vapor pressure. Lighter compounds were mainly in the gaseous phase, while heavier compounds were mainly associated to the particulate phase. These results are comparable to literature reports for ambient air or wood combustion emission studies (Albinet et al., 2007, Albinet et al., 2008, Pankow, 1987, Shen et al., 2012a, Tomaz et al., 2016)

and references therein). Besides, other parameters like the molecular structure could have a strong importance in the gas/particle partitioning as shown by the singular behaviour observed for some OPAHs and NPAHs (*e.g.* acenaphthenequinone) (Tomaz et al., 2016).

Overall, results obtained in both output conditions (either nominal or reduced) did not differ significantly. However, in reduced output experiments, the low concentration levels in VCF and CF induced a disruption of the results obtained for some compounds (*e.g.* 1,4-anthraquinone, 2-nitro-9-fluorenone, 3-nitrofluoranthene, 6-nitrochrysene and 1,8-dinitropyrene).

From E until VCF, results showed that SVOCs condensed rapidly on pre-existing particles due to the high temperature decrease (from 200-350 °C to less than 50 °C in VCF). Lighter compounds (MW≤180-192 g mol^{-1}) remained only in the gaseous phase while heavier compounds (MW≥273 g mol^{-1}, in nominal output, and MW≥230 g mol^{-1}, in reduced output) remained associated to the particulate phase. The differences between nominal and reduced outputs, observed for the heavier compounds, were related to the lower emission smoke temperature in the latter condition (≤275 °C for the reduced output *vs*. ≥340 °C for the nominal output). Because of dilution, re-evaporation from the particulate phase to the gaseous phase could also occur between VCF and CF.

3.2.2. Evolution of the total PAH, OPAH and NPAH emission factors from E until CF

The evolution of the total EFs (or equivalent EFs in VCF and CF) of parent PAHs, NPAHs and OPAHs (sum of the individual EFs), from the emission until close field, is shown in Figure 2.

Overall, for PAHs, the EF Σ_{37}PAHs slightly decreased from E until CF. At the same time, for NPAHs and OPAHs, the results show a strong and significant increase of EF Σ_{31}NPAHs and EF Σ_{27}OPAHs from E until CF. This was clearly observed for both, NPAHs and OPAHs, with the 5* RWS in nominal output conditions and, for NPAHs, with the 4* and 5* RWS in reduced output conditions. These results suggest that a fast oxidation process occurred between E and CF (about 10 seconds after emission), and notably between VCF and CF, resulting in higher equivalent OPAH and NPAH EFs determined in VCF and CF. The oxygen content of the wood combustion effluent from the emission point until its insertion in ambient air changed only in a few seconds, resulting in the rapid formation of OPOA (oxidized primary organic aerosol).

3.2.3. Study of PAH ratio-ratio plots

PAH ratio-ratio plots are usually used for PAH source apportionment studies (Robinson et al., 2006). Figure 3 shows the PAH ratio-ratio plot of Benzo[b+k]Fluoranthene/Indeno[1,2,3-cd]Pyrene *vs* Benzo[g,h,i]Perylene/Indeno[1,2,3-cd]Pyrene, (B[b+k]F/Ind[1,2,3-cd]P) *vs* (B[g,h,i]P/Ind[1,2,3-cd]P), obtained at the E, VCF (both measurement methods, M1 and M2) and CF for all experiments (both nominal and reduced output). These compounds are commonly used as PAH molecular markers (Albinet et al., 2007, Marchand et al., 2004, Robinson et al., 2006). Four different combustion sources are also displayed on the PAH ratio-ratio plots, including

biomass burning (Fine et al., 2004a), green grass waste burning (Piot, 2011), vehicular (El Haddad et al., 2009) and industrial emissions (graphite material production) (Golly et al., 2015). In Figure 3A, only the particulate phase is considered, while Figure 3B shows the results taking into account both the gaseous, and particulate phases.

For the particulate phase only (Figure 3A), the results obtained showed an evolution of the PAH ratio-ratio from E to CF. Finally, the values in CF were close to those calculated using the literature data for biomass burning and green waste burning. Interestingly, considering both particulate, and gaseous phases (Figure 3B), the PAH ratio-ratio values in E and VCF were similar. B[g,h,i]P and Ind[1,2,3-cd]P were only associated to the particulate phase at all sampling locations (E, VCF and CF), while B[b+k]F was in the gaseous phase at the emission and shifted to the particulate phase in VCF and CF. This phenomenon was due to condensation processes linked to the temperature decrease (Figures 1, S2, S3, S4). Considering both the gaseous, and the particulate phases, the ratio B[b+k]F/Ind[1,2,3-cd]P was not impacted by the condensation process (contribution of SVOCs was already included). It resulted in similar values for both the E and VCF sampling locations.

From VCF until CF, the PAH ratio-ratio evolved with a strong decrease of the B[g,h,i]P/Ind[1,2,3-cd]P ratio. Since B[g,h,i]P is known to be a highly reactive PAH, while Ind[1,2,3-cd]P is more stable (Esteve et al., 2006, Ringuet et al., 2012), a fast oxidation process from VCF until CF could explain the observed changes. B[k]F and B[b]F (and notably the latter one) are stable compounds in the presence of oxidants such as OH (Esteve et al., 2006, Ringuet et al., 2012), explaining why the ratio B[b+k]F/Ind[1,2,3-cd]P remained quite constant between VCF and CF.

The PAH ratio-ratio data in the literature has been derived by using tunnel dilution systems or open fire experiments. The literature values could as well be affected by a fast oxidation process like in our study, explaining why our CF PAH ratio-ratio values were similar to literature data for biomass burning and green waste burning.

All these results tended to prove that fast oxidation processes occurred between E to CF (and notably between VCF and CF) changing in a few seconds the oxidation state of the wood combustion effluent and causing the formation of OPOA.

3.2.4. Evolution from E until CF of the ratios PAH derivatives/Parent PAHs

The evolution, from E until CF, of the PAH derivatives/parent PAHs concentration ratios has been investigated for all combustion experiments. These ratios are usually used as indicators of the secondary formation of OPAHs and NPAHs from PAH atmospheric photooxidation processes (Alam et al., 2014).

Figure 4 shows, as an example, the results obtained for phenanthrene (6H-dibenzo[b,d]pyran-6-one, biphenyl-2-2′-dicarboxaldehyde, 9,10-phenanthrenequinone and 9-phenanthrene carboxaldehyde) and acenaphthene OPAH derivatives (1,8-naphthalic anhydride, 1-acenaphthenone and acenaphthenequinone) (both, gaseous and particulate phases considered). Some of these compounds have been reported as typical by-products of PAH photooxidation resulting in SOA formation [for phenanthrene: 6H-dibenzo[b,d]pyran-6-one, biphenyl-2-2′-dicarboxaldehyde, 9,10-phenanthrenequinone ; for acenaphthene: 1,8-naphthalic anhydride (and also for acenaphthylene, PAH not analyzed here) and 1-acenaphthenone] (Lee and Lane, 2010, Lee et al., 2012, Perraudin et al., 2007, Zhou and Wenger, 2013a, 2013b).

OPAH derivatives/parent PAHs ratios increased significantly from E until CF highlighting a PAH oxidation process. Similar results were obtained for almost all the other PAHs derivatives and parent PAHs. As already shown before, fast oxidation seemed to occur mainly between VCF and CF. The structure of the vertical part of the fire gallery (Figure S1) provided ideal mixing and reaction conditions between PAHs and oxidants ($H^{\cdot}$, $O^{\cdot}$ and $OH^{\cdot}$ free radicals) emitted by the flames. As mentioned before, the oxidation process was particularly obvious during nominal output experiments. In these flaming combustion conditions, emission of oxidants and smoke temperature were higher. Previous studies have shown that the formation of OPAHs is increased at higher temperatures (Fitzpatrick et al., 2007, Orasche et al., 2013).

Therefore, this suggested that fast oxidation processes occurred between E and CF (and especially between VCF and CF), notably in nominal output conditions, modifying the oxidation state of the wood combustion effluent in a few seconds and resulting in the formation of OPOA including toxic compounds like OPAHs and, to a lesser extent, NPAHs.

Figures 5 and S5 show the evolution of individual PAH derivatives/parent PAHs ratios from E until CF (both, gaseous and particulate phases considered). The results obtained for naphthalene, acenaphthene and benz[a]anthracene are presented as examples The increase of the ratios highlights fast oxidation processes from E to CF. Some of these OPAHs and NPAHs have been previously identified as typical secondary pollutants formed from photooxidation of the parent PAHs in atmospheric conditions (*i.e.* by reaction with atmospheric oxidants such as O_3, OH, NO_2 or NO_3). They include 1- and 2-nitronapthalene, 1,4-naphtoquinone, 2-formyl-trans-cinnamaledhyde and phthaldialdehyde for naphthalene (Chan et al., 2009, Lee and Lane, 2009,

Nishino et al., 2009, Sasaki et al., 1997), and 1,8-naphthalic anhydride and 1-acenaphthenone for acenaphthene (Zhou and Wenger, 2013b).

Besides, the ratios of PAH derivatives/benz[a]anthracene (namely, 7-nitrobenz[a]anthracene and benz[a]anthracene-7,12-dione) showed two different trends (Figure S5). The increase of the 7-nitrobenz[a]anthracene/benz[a]anthracene ratio from E to CF is in agreement with its probable secondary formation (Ringuet et al., 2012). For benz[a]anthracene-7,12-dione, the ratio remained constant. This result suggests that benz[a]anthracene-7,12-dione is prevalently part of primary emission by wood combustion. This is consistent with the results of Ringuet et al. (2012), who showed that benz[a]anthracene-7,12-dione was formed by the reaction of benz[a]anthracene with O_3 but not in the presence of $OH^{\cdot}$ radicals. In fact, during combustion experiments, there was no O_3 and only $O^{\cdot}$, $H^{\cdot}$ and $OH^{\cdot}$ free radicals could be emitted by the flames. Therefore, no formation of benz[a]anthracene-7,12-dione could occur. Additionally, (Keyte et al., 2016) showed that this compound had a primary origin in ambient air. This result supports the argument that the formation of typical by-products from PAH oxidation, observed from E to CF, was major and not a consequence of sampling artefacts or analytical drift.

4. Conclusions

The evolution, in controlled real conditions, of the aerosol emitted by two different residential log wood stoves (old and modern technologies) from emission until ambient air introduction was studied. Toxic substances, primary and/or secondary formed, such as polycyclic aromatic hydrocarbons (PAH) and their nitrated and oxygenated derivatives, were especially investigated. Results obtained showed that emission factors (EF) of Σ_{37}PAHs and Σ_{27}Oxy-PAHs were in the same range and similar to those reported in literature. EF of nitro-PAHs (Σ_{31} compounds), poorly

documented in the literature, were 2 to 4 orders of magnitude lower linked to the low temperature and the low NO_2 emission from wood combustion processes. The study of the gas/particle partitioning of these semi-volatile organic compounds showed a fast condensation on pre-existing particles due to the high temperature decrease between emission and very close field (from about 200-350 °C to less than 50 °C). Interestingly, from emission to ambient air introduction, an increase of equivalent EF of PAH derivatives was observed. The study of PAH ratio-ratio plots, commonly used for source evaluation, and PAH derivative/parent PAH ratios, calculated also for typical compounds of PAH SOA formation, showed that the oxygen content of the wood combustion effluent changed in a few seconds. This was especially obvious for nominal output combustion conditions due to the large emission of oxidant radicals from the flames. These processes resulted in the fast formation of OPOA. The differences of chemical profiles observed between measurements performed directly at the emission and in close field (after dilution to simulate ambient air concentrations) have an impact on the emission inventories currently used and then, this kind of chemical processes should be taken into account in air quality models.

Acknowledgements

This work was supported by the French Ministry of Environment (MEEM) and ADEME (French Environment and Energy Management Agency). Authors thank Patrick Bodu for the graphical abstract design and Dawn Avalon Zammit for useful English corrections.

Appendix A. Supplementary data

Supplementary data associated with this article can be found online at http://www.journals.elsevier.com/atmospheric-environment.

References

Alam, M. S.,Delgado-Saborit, J. M.,Stark, C. and Harrison, R. M., 2014. Investigating PAH relative reactivity using congener profiles, quinone measurements and back trajectories. Atmospheric Chemistry and Physics 14, 2467-2477.

Albinet, A.,Leoz-Garziandia, E.,Budzinski, H. and Villenave, E., 2006. Simultaneous analysis of oxygenated and nitrated polycyclic aromatic hydrocarbons on standard reference material 1649a (urban dust) and on natural ambient air samples by gas chromatography-mass spectrometry with negative ion chemical ionisation. Journal of Chromatography A 1121, 106-113.

Albinet, A.,Leoz-Garziandia, E.,Budzinski, H. and Villenave, E., 2007. Polycyclic aromatic hydrocarbons (PAHs), nitrated PAHs and oxygenated PAHs in ambient air of the Marseilles area (South of France): Concentrations and sources. Science of the Total Environment 384, 280-292.

Albinet, A.,Leoz-Garziandia, E.,Budzinski, H.,Villenave, E. and Jaffrezo, J. L., 2008. Nitrated and oxygenated derivatives of polycyclic aromatic hydrocarbons in the ambient air of two French alpine valleys. Part 1: Concentrations, sources and gas/particle partitioning. Atmospheric Environment 42, 43-54.

Albinet, A.,Tomaz, S. and Lestremau, F., 2013. A really quick easy cheap effective rugged and safe (QuEChERS) extraction procedure for the analysis of particle-bound PAHs in ambient air and emission samples. Science of the Total Environment 450-451, 31-38.

Albinet, A.,Nalin, F.,Tomaz, S.,Beaumont, J. and Lestremau, F., 2014. A simple QuEChERS-like extraction approach for molecular chemical characterization of organic aerosols: application to nitrated and oxygenated PAH derivatives (NPAH and OPAH) quantified by GC–NICIMS. Analytical and Bioanalytical Chemistry 406, 3131-3148.

Arey, J.,Zielinska, B.,Atkinson, R.,Winer, A. M.,Ramdhal, T. and Pitts Jr, J. N., 1986. The formation of nitro-PAH from the gas-phase reactions of fluoranthene and pyrene with the OH radical in the presence of NO_x. Atmospheric Environment 20, 2239-2345.

Besombes, J.-L.,Maitre, A.,Patissier, O.,Marchand, N.,Chevron, N.,Stoklov, M. and Masclet, P., 2001. Particulate PAHs observed in the surrounding of a municipal incinerator. Atmospheric Environment 35, 6093-6104.

Bruns, E. A.,Krapf, M.,Orasche, J.,Huang, Y.,Zimmermann, R.,Drinovec, L.,Močnik, G.,El-Haddad, I.,Slowik, J. G.,Dommen, J.,Baltensperger, U. and Prévôt, A. S. H., 2015. Characterization of primary and secondary wood combustion products generated under different burner loads. Atmospheric Chemistry and Physics 15, 2825-2841.

CEN (European Comittee for Standardization), Residential solid fuel burning appliances Part 1 General requirements and test methods. In 2013.

Chan, A. W. H.,Kautzman, K. E.,Chhabra, P. S.,Surratt, J. D.,Chan, M. N.,Crounse, J. D.,Kürten, A.,Wennberg, P. O.,Flagan, R. C. and Seinfeld, J. H., 2009. Secondary organic aerosol formation from photooxidation of naphthalene and alkylnaphthalenes: implications for oxidation of intermediate volatility organic compounds (IVOCs). Atmospheric Chemistry and Physics 9, 3049-3060.

Chen, C.-L.,Kacarab, M.,Tang, P. and Cocker Iii, D. R., 2016. SOA formation from naphthalene, 1-methylnaphthalene, and 2-methylnaphthalene photooxidation. Atmospheric Environment 131, 424-433.

CITEPA, 2015. Inventaire des émissions de polluants atmosphériques et de gaz à effet de serre en France – Séries sectorielles et analyses étendues. CITEPA (Centre Interprofessionnel Technique d'Etudes de la Pollution Atmosphérique): http://www.citepa.org/images/III-1_Rapports_Inventaires/secten_avril2015_sec.pdf.

Denier van der Gon, H. A. C.,Bergström, R.,Fountoukis, C.,Johansson, C.,Pandis, S. N.,Simpson, D. and Visschedijk, A. J. H., 2015. Particulate emissions from residential wood combustion in Europe – revised estimates and an evaluation. Atmospheric Chemistry and Physics 15, 6503-6519.

Durant, J. L.,Busby Jr, W. F.,Lafleur, A. L.,Penman, B. W. and Crespi, C. L., 1996. Human cell mutagenicity of oxygenated, nitrated and unsubstituted polycyclic aromatic hydrocarbons associated with urban aerosols. Mutation Research-Genetic Toxicology 371, 123-157.

Durant, J. L.,Lafleur, A. L.,Plummer, E. F.,Taghizadeh, K.,Busby, W. F. and Thilly, W. G., 1998. Human lymphoblast mutagens in urban airborne particles. Environmental Science & Technology 32, 1894-1906.

El Haddad, I.,Marchand, N.,Dron, J.,Temime-Roussel, B.,Quivet, E.,Wortham, H.,Jaffrezo, J. L.,Baduel, C.,Voisin, D.,Besombes, J. L. and Gille, G., 2009. Comprehensive primary particulate organic characterization of vehicular exhaust emissions in France. Atmospheric Environment 43, 6190-6198.

Environmental Health Criteria (EHC) 229, 2003. Selected nitro- and nitro-oxy-polycyclic aromatic hydrocarbons. WHO Library: http://whqlibdoc.who.int/ehc/WHO_EHC_229.pdf.

Esteve, W.,Budzinski, H. and Villenave, E., 2006. Relative rate constants for the heterogeneous reactions of NO_2 and OH radicals with polycyclic aromatic hydrocarbons adsorbed on carbonaceous particles. Part 2: PAHs adsorbed on diesel particulate exhaust SRM 1650a. Atmospheric Environment 40, 201-211.

European Official Journal, Directive 2004/107/CE of the European Parliament and of the Council of 15 December 2004 relating to arsenic, cadmium, mercury, nickel and polycyclic aromatic hydrocarbons in ambient air. In *Official Journal*, 2004; Vol. L23, pp 3-16.

Favez, O.,Cachier, H.,Sciare, J.,Sarda-Estève, R. and Martinon, L., 2009. Evidence for a significant contribution of wood burning aerosols to $PM_{2.5}$ during the winter season in Paris, France. Atmospheric Environment 43, 3640-3644.

Favez, O.,El Haddad, I.,Piot, C.,Boréave, A.,Abidi, E.,Marchand, N.,Jaffrezo, J. L.,Besombes, J. L.,Personnaz, M. B.,Sciare, J.,Wortham, H.,George, C. and D'Anna, B., 2010. Inter-comparison of source apportionment models for the estimation of wood burning aerosols during wintertime in an Alpine city (Grenoble, France). Atmospheric Chemistry and Physics 10, 5295-5314.

Fine, P. M.,Cass, G. R. and Simoneit, B. R. T., 2001. Chemical characterization of fine particle emissions from fireplace combustion of woods grown in the Northeastern United States. Environmental Science & Technology 35, 2665-2675.

Fine, P. M.,Cass, G. R. and Simoneit, B. R. T., 2002. Chemical characterization of fine Particle emissions from the fireplace combustion of woods grown in the Southern United States. Environmental Science & Technology 36, 1442-1451.

Fine, P. M.,Cass, G. R. and Simoneit, B. R. T., 2004a. Chemical characterization of fine particle emissions from the wood stove combustion of prevalent United States tree species. Environmental Engineering Science 21, 705-721.

Fine, P. M.,Cass, G. R. and Simoneit, B. R. T., 2004b. Chemical characterization of fine particle emissions from the fireplace combustion of wood types grown in the Midwestern and Western United States. Environmental Engineering Science 21, 387-409.

Fitzpatrick, E. M.,Ross, A. B.,Bates, J.,Andrews, G.,Jones, J. M.,Phylaktou, H.,Pourkashanian, M. and Williams, A., 2007. Emission of oxygenated species from the combustion of pine wood and its relation to soot formation. Process Safety and Environmental Protection 85, 430-440.

Fraboulet, I., 2012. PEREN^{2}BOIS: Evaluation technico-économique des meilleures techniques disponibles de réduction des émissions de poussières fines et de composés organiques pour les appareils de combustion domestique utilisant la biomasse (French language). ADEME: http://www.ineris.fr/centredoc/peren2bois-1357814186.pdf.

Golly, B.,Brulfert, G.,Berlioux, G.,Jaffrezo, J. L. and Besombes, J. L., 2015. Large chemical characterisation of PM_{10} emitted from graphite material production: Application in source apportionment. Science of the Total Environment 538, 634-643.

Gonçalves, C.,Alves, C.,Evtyugina, M.,Mirante, F. t.,Pio, C.,Caseiro, A.,Schmidl, C.,Bauer, H. and Carvalho, F., 2010. Characterisation of PM_{10} emissions from woodstove combustion of common woods grown in Portugal. Atmospheric Environment 44, 4474-4480.

Goriaux, M.,Jourdain, B.,Temime, B.,Besombes, J.-L.,Marchand, N.,Albinet, A.,Leoz-Garziandia, E. and Wortham, H., 2006. Field comparison of particulate PAH measurements

using a low flow denuder device and conventional sampling systems. Environmental Science & Technology 40, 6398-6404.

Gullett, B. K.,Touati, A. and Hays, M. D., 2003. PCDD/F, PCB, HxCBz, PAH, and PM emission factors for fireplace and woodstove combustion in the San Francisco Bay region. Environmental Science & Technology 37, 1758-1765.

Herich, H.,Gianini, M. F. D.,Piot, C.,Močnik, G.,Jaffrezo, J. L.,Besombes, J. L.,Prévôt, A. S. H. and Hueglin, C., 2014. Overview of the impact of wood burning emissions on carbonaceous aerosols and PM in large parts of the Alpine region. Atmospheric Environment 89, 64-75.

IARC, 2010. Some non-heterocyclic polycyclic aromatic hydrocarbons and some related exposures. Lyon (France), Vol. 92.

IARC, 2012. A review of human carcinogens: Some chemicals in industrial and consumer products, food contaminants and flavourings, and water chlorination by-products. Lyon (France), Vol. 101.

IARC, 2013. Diesel and gasoline engine exhaust and some nitroarenes. Lyon (France), Vol. 105.

Iinuma, Y.,Bruggemann, E.,Gnauk, T.,Muller, K.,Andreae, M. O.,Helas, G.,Parmar, R. and Herrmann, H., 2007. Source characterization of biomass burning particles: the combustion of selected European conifers, African hardwood, savanna grass, and German and Indonesian peat. Journal of Geophysical Research-Atmospheres 112.

Kautzman, K. E.,Surratt, J. D.,Chan, M. N.,Chan, A. W. H.,Hersey, S. P.,Chhabra, P. S.,Dalleska, N. F.,Wennberg, P. O.,Flagan, R. C. and Seinfeld, J. H., 2010. Chemical composition of gas- and aerosol-phase products from the photooxidation of naphthalene. The Journal of Physical Chemistry A 114, 913-934.

Keyte, I. J.,Harrison, R. M. and Lammel, G., 2013. Chemical reactivity and long-range transport potential of polycyclic aromatic hydrocarbons - a review. Chemical Society Reviews 42, 9333-9391.

Keyte, I. J.,Albinet, A. and Harrison, R. M., 2016. On-road traffic emissions of polycyclic aromatic hydrocarbons and their oxy- and nitro- derivative compounds measured in road tunnel environments. Science of the Total Environment.

Lee, J. and Lane, D. A., 2010. Formation of oxidized products from the reaction of gaseous phenanthrene with the OH radical in a reaction chamber. Atmospheric Environment 44, 2469-2477.

Lee, J. Y. and Lane, D. A., 2009. Unique products from the reaction of naphthalene with the hydroxyl radical. Atmospheric Environment 43, 4886-4893.

Lee, J. Y.,Lane, D. A.,Heo, J. B.,Yi, S.-M. and Kim, Y. P., 2012. Quantification and seasonal pattern of atmospheric reaction products of gas phase PAHs in $PM_{2.5}$. Atmospheric Environment 55, 17-25.

Maenhaut, W.,Vermeylen, R.,Claeys, M.,Vercauteren, J.,Matheeussen, C. and Roekens, E., 2012. Assessment of the contribution from wood burning to the PM_{10} aerosol in Flanders, Belgium. Science of the Total Environment 437, 226-236.

Marchand, N.,Besombes, J. L.,Chevron, N.,Masclet, P.,Aymoz, G. and Jaffrezo, J. L., 2004. Polycyclic aromatic hydrocarbons (PAHs) in the atmospheres of two French alpine valleys: sources and temporal patterns. Atmospheric Chemistry and Physics 4, 1167-1181.

Nishino, N.,Arey, J. and Atkinson, R., 2009. Formation and Reactions of 2-Formylcinnamaldehyde in the OH Radical-Initiated Reaction of Naphthalene. Environmental Science & Technology 43, 1349-1353.

Nussbaumer, T.,Klippel, N. and Johansson, L. In *Survey on measurements and emission factors on particulate matter from biomass combustion in IEA countries*, 16th European Biomass Conference and Exhibition, Valencia (Spain), 2008; Valencia (Spain), 2008.

Orasche, J.,Seidel, T.,Hartmann, H.,Schnelle-Kreis, J.,Chow, J. C.,Ruppert, H. and Zimmermann, R., 2012. Comparison of emissions from wood combustion. Part 1: emission factors and characteristics from different small-scale residential heating appliances considering particulate matter and polycyclic aromatic hydrocarbon (PAH)-related toxicological potential of particle-bound organic species. Energy & Fuels 26, 6695-6704.

Orasche, J.,Schnelle-Kreis, J.,Schön, C.,Hartmann, H.,Ruppert, H.,Arteaga-Salas, J. M. and Zimmermann, R., 2013. Comparison of emissions from wood combustion . Part 2: Impact of combustion conditions on emission factors and characteristics of particle-bound organic species and polycyclic aromatic hydrocarbon (PAH)-related toxicological potential. Energy & Fuels 27, 1482-1491.

Pankow, J. F., 1987. Review and comparative analysis of the theories on partitioning between the gas and aerosol particulate phases in the atmosphere. Atmospheric Environment (1967) 21, 2275-2283.

Pedersen, D. U.,Durant, J. L.,Penman, B. W.,Crespi, C. L.,Hemond, H. F.,Lafleur, A. L. and Cass, G. R., 2004. Human-cell mutagens in respirable airborne particles in the northeastern

United States. 1. Mutagenicity of fractionated samples. Environmental Science & Technology 38, 682-689.

Pedersen, D. U.,Durant, J. L.,Taghizadeh, K.,Hemond, H. F.,Lafleur, A. L. and Cass, G. R., 2005. Human cell mutagens in respirable airborne particles from the Northeastern United States. 2. Quantification of mutagens and other organic compounds. Environmental Science & Technology 39, 9547-9560.

Perraudin, E.,Budzinski, H. and Villenave, E., 2007. Identification and quantification of primary ozonation products of phenanthrene and anthracene adsorbed on silica particles. Atmospheric Environment 41, 6005-6017.

Piot, C. 2011. Polluants atmosphériques organiques particulaires en Rhône-Alpes: caractérisation chimique et sources d'émission. PhD thesis. Université de Grenoble (French language).

Pye, H. O. T. and Seinfeld, J. H., 2010. A global perspective on aerosol from low-volatility organic compounds. Atmospheric Chemistry and Physics 10, 4377-4401.

Ringuet, J.,Albinet, A.,Leoz-Garziandia, E.,Budzinski, H. and Villenave, E., 2012. Reactivity of polycyclic aromatic compounds (PAHs, NPAHs and OPAHs) adsorbed on natural aerosol particles exposed to atmospheric oxidants. Atmospheric Environment 61, 15-22.

Robinson, A. L.,Subramanian, R.,Donahue, N. M.,Bernardo-Bricker, A. and Rogge, W. F., 2006. Source apportionment of molecular markers and organic aerosol-1. Polycyclic aromatic hydrocarbons and methodology for data visualization. Environmental Science & Technology 40, 7803-7810.

Rogge, W. F.,Hildemann, L. M.,Mazurek, M. A.,Cass, G. R. and Simoneit, B. R. T., 1993. Sources of fine organic aerosol. 2. Noncatalyst and catalyst-equipped automobiles and heavy-duty diesel trucks. Environmental Science & Technology 27, 636-651.

Rogge, W. F.,Hildemann, L. M.,Mazurek, M. A.,Cass, G. R. and Simoneit, B. R. T., 1998. Sources of fine organic aerosol. 9. Pine, oak and synthetic log combustion in residential fireplaces. Environmental Science & Technology 32, 13-22.

Sasaki, J.,Aschmann, S. M.,Kwok, E. S. C.,Atkinson, R. and Arey, J., 1997. Products of the gas-phase OH and NO_3 radical-initiated reactions of naphthalene. Environmental Science & Technology 31, 3173-3179.

Schauer, J. J.,Kleeman, M. J.,Cass, G. R. and Simoneit, B. R. T., 1999. Measurement of emissions from air pollution sources. 2. C-1 through C-30 organic compounds from medium duty diesel trucks. Environmental Science & Technology 33, 1578-1587.

Schauer, J. J.,Kleeman, M. J.,Cass, G. R. and Simoneit, B. R. T., 2001. Measurement of emissions from air pollution sources. 3. C-1-C-29 organic compounds from fireplace combustion of wood. Environmental Science & Technology 35, 1716-1728.

Schauer, J. J.,Kleeman, M. J.,Cass, G. R. and Simoneit, B. R. T., 2002. Measurement of emissions from air pollution sources. 5. C-1-C-32 organic compounds from gasoline-powered motor vehicles. Environmental Science & Technology 36, 1169-1180.

Scheepers, P. T. J. and Bos, R. P., 1992. Combustion of diesel fuel from a toxicological perspective. International Archives of Occupational and Environmental Health 64, 149-161.

Shakya, K. M. and Griffin, R. J., 2010. Secondary organic aerosol from photooxidation of polycyclic aromatic hydrocarbons. Environmental Science & Technology 44, 8134-8139.

Shen, G.,Tao, S.,Wei, S.,Zhang, Y.,Wang, R.,Wang, B.,Li, W.,Shen, H.,Huang, Y.,Chen, Y.,Chen, H.,Yang, Y.,Wang, W.,Wang, X.,Liu, W. and Simonich, S. L. M., 2012a. Emissions of parent, nitro, and oxygenated polycyclic aromatic hydrocarbons from residential wood combustion in rural China. Environmental Science & Technology 46, 8123-8130.

Shen, G.,Wei, S.,Zhang, Y.,Wang, R.,Wang, B.,Li, W.,Shen, H.,Huang, Y.,Chen, Y.,Chen, H.,Wei, W. and Tao, S., 2012b. Emission of oxygenated polycyclic aromatic hydrocarbons from biomass pellet burning in a modern burner for cooking in China. Atmospheric Environment 60, 234-237.

Tomaz, S.,Shahpoury, P.,Jaffrezo, J.-L.,Lammel, G.,Perraudin, E.,Villenave, E. and Albinet, A., 2016. One-year study of polycyclic aromatic compounds at an urban site in Grenoble (France): Seasonal variations, gas/particle partitioning and cancer risk estimation. Science of the Total Environment 565, 1071-1083.

Verlhac, S. and Albinet, A., 2015. European Interlaboratory Comparison for the analysis of PAH in ambient air. LCSQA: http://www.lcsqa.org/rapport/2015/ineris/european-interlaboratory-comparison-for-the-analysis-of-pah-in-ambient-air.

Viana, M.,Alastuey, A.,Querol, X.,Guerreiro, C.,Vogt, M.,Colette, A.,Collet, S.,Albinet, A.,Fraboulet, I.,Lacome, J.-M.,Tognet, F. and de Leeuw, F., 2016. Contribution of residential combustion to ambient air pollution and greenhouse gas emissions. EEA: http://acm.eionet.europa.eu/reports/ETCACM_TP_2015_1_residential_combustion.

Vicente, E.,Vicente, A.,Musa Bandowe, B. and Alves, C., 2015. Particulate phase emission of parent polycyclic aromatic hydrocarbons (PAHs) and their derivatives (alkyl-PAHs, oxygenated-

PAHs, azaarenes and nitrated PAHs) from manually and automatically fired combustion appliances. Air Quality, Atmosphere & Health, 1-16.

Zhang, H. and Ying, Q., 2011. Secondary organic aerosol formation and source apportionment in Southeast Texas. Atmospheric Environment 45, 3217-3227.

Zhou, S. and Wenger, J. C., 2013a. Kinetics and products of the gas-phase reactions of acenaphthylene with hydroxyl radicals, nitrate radicals and ozone. Atmospheric Environment 75, 103-112.

Zhou, S. and Wenger, J. C., 2013b. Kinetics and products of the gas-phase reactions of acenaphthene with hydroxyl radicals, nitrate radicals and ozone. Atmospheric Environment 72, 97-104.

Zielinska, B.,Sagebiel, J.,McDonald, J. D.,Whitney, K. and Lawson, D. R., 2004. Emission rates and comparative chemical composition from selected in-use diesel and gasoline-fueled Vehicles. Journal of the Air & Waste Management Association 54, 1138-1150.

Zielinska, B., 2008. Analysis of semi-volatile compounds by GC/MS. Desrt Research Institute: http://www.epa.gov/ttnamti1/files/ambient/pm25/spec/DRISOPSVOC92408.pdf.

Table 1. Summary of the wood burning experiment conditions and concentrations of $PM_{2.5}$ (concentrations on dry gas basis 95 calculated for normal conditions and at actual O_2 concentration levels).

# [a]	RWS	Output	Wood load (kg) (number of logs) [b]	Combustion duration (h)	Wood stove emission flow ($Nm^3\ h^{-1}$) [c]	Ambient temperature (°C)	Dilution Factor [d]		Smoke temperature (°C)			$PM_{2.5}$ (solid fraction) ($mg\ Nm^{-3}$) [h]			$PM_{2.5}$ (solid + condensable fractions) ($mg\ Nm^{-3}$) [h]		
							VCF	CF	E [e]	VCF [f]	CF [g]	E	VCF	CF	E	VCF	CF
1	4*	Nominal	4.05 (2)	0.95	34.4	10.5	21	668	367	37	12	136	5.5	0.18	201	8.6	0.28
2	4*	Reduced	3.18 (2)	1.1	26.6	13.5	16	639	275	33	15	73	2.7	0.18	301	5.8	0.60
3	4*	Nominal	4.03 (2)	1.03	29.3	13.0	20	777	358	35	15	135	3.6	0.16	191	7.8	0.29
4	5*	Nominal	2.81 (2)	0.75	30.3	9.2	16	596	362	50	11	279	20.8	0.58	396	27.8	0.72
5	5*	Nominal	3.07 (2)	0.87	30.9	10.0	16	580	340	49	12	275	13.8	0.32	335	18.8	0.54
6	5*	Reduced	2.11 (2)	1.18	18.6	9.3	24	555	187	24	11	101	13.0	0.27	647	29.6	0.74*

[a] Experiment number.
[b] Beech, 12 % moisture.
[c] Dry gas.
[d] Dilution factors determined using air flow or concentration ratios of the gaseous compounds (CO, CO_2, NO_x) measured at each sampling point. Results obtained were all in agreement if no probe/analyzer dysfunction or overload was observed.
[e] E: emission.
[f] VCF: very close field.
[g] CF: close field.
[h] Concentrations on dry gas basis calculated for normal conditions (273.15 K, 1.013×10^5 Pa).
* Doubtful value.

Table 2. Average emission factors of parent PAHs (mg kg^{-1}, dry mass basis) for both RWS (4* and 5*) in nominal and reduced output conditions. Measurements performed at the emission sampling location

Compounds	*4* RWS*			*5* RWS*		
	Nominal output		*Reduced output*	*Nominal output*		*Reduced output*
Naphthalene	5.0×10^{1}	(3.3×10^{1})[a]	9.5×10^{0}	9.7×10^{1}	(1.4×10^{1})	8.6×10^{1}
Acenaphthene	2.3×10^{-1}	(3.2×10^{-1})	8.7×10^{-2}	5.9×10^{-1}	(3.8×10^{-1})	1.5×10^{0}
Fluorene	2.1×10^{0}	(6.2×10^{-1})	1.2×10^{0}	4.0×10^{0}	(2.3×10^{0})	4.1×10^{0}
Phenanthrene	2.3×10^{1}	(1.7×10^{1})	3.2×10^{0}	4.3×10^{1}	(3.4×10^{1})	2.9×10^{1}
Anthracene	2.1×10^{0}	(1.1×10^{0})	5.7×10^{-1}	9.0×10^{0}	(7.3×10^{0})	5.3×10^{0}
Fluoranthene	4.7×10^{0}	(3.3×10^{0})	7.8×10^{-1}	1.8×10^{1}	(1.3×10^{1})	5.8×10^{0}
Pyrene	7.9×10^{0}	(8.0×10^{0})	8.3×10^{-1}	1.9×10^{1}	(1.5×10^{1})	4.3×10^{0}
Retene	1.7×10^{-1}	(2.3×10^{-1})	8.5×10^{-2}	2.4×10^{0}	(1.2×10^{0})	9.7×10^{-1}
Benz[a]anthracene	6.2×10^{-1}	(4.6×10^{-1})	1.7×10^{-1}	4.7×10^{0}	(2.1×10^{0})	1.7×10^{0}
Chrysene	5.6×10^{-1}	(4.2×10^{-1})	8.7×10^{-2}	3.5×10^{0}	(2.1×10^{0})	7.7×10^{-1}
Benzo[e]pyrene	3.7×10^{-1}	(1.4×10^{-1})	8.1×10^{0}	4.0×10^{0}	(4.2×10^{0})	7.7×10^{-1}
Benzo[b]fluoranthene	6.3×10^{-1}	(4.8×10^{-1})	1.1×10^{-1}	2.2×10^{0}	(1.1×10^{0})	6.8×10^{-1}
Benzo[k]fluoranthene	2.7×10^{-1}	(2.1×10^{-1})	5.3×10^{-2}	1.4×10^{0}	(5.0×10^{-1})	3.5×10^{-1}
Benzo[a]pyrene	6.1×10^{-1}	(5.0×10^{-1})	1.3×10^{-1}	3.8×10^{0}	(1.5×10^{0})	8.6×10^{-1}
Benzo[g,h,i]perylene	2.0×10^{-1}	(2.2×10^{-1})	7.2×10^{-3}	2.4×10^{0}	(1.3×10^{-2})	6.7×10^{-1}
Dibenz[a,h]anthracene	1.2×10^{-2}	(1.2×10^{-2})	6.8×10^{-4}	9.5×10^{-2}	(1.3×10^{-1})	5.6×10^{-2}
Indeno[1,2,3-cd]pyrene	1.6×10^{-1}	(1.7×10^{-1})	7.9×10^{-3}	2.1×10^{0}	(1.5×10^{-1})	4.1×10^{-1}
Coronene	8.9×10^{-2}	(6.4×10^{-2})	1.2×10^{-2}	4.7×10^{-1}	(6.2×10^{-1})	2.0×10^{-1}
2-Methylnaphthalene	2.7×10^{0}	(2.2×10^{0})	1.9×10^{0}	1.1×10^{1}	(5.3×10^{0})	7.5×10^{0}
1-Methylfluorene	1.5×10^{-1}	(1.1×10^{-1})	2.2×10^{-1}	5.5×10^{-1}	(6.0×10^{-1})	3.9×10^{-1}
3-Methylphenanthrene	1.9×10^{-1}	(1.6×10^{-1})	1.3×10^{-1}	6.0×10^{-1}	(6.2×10^{-1})	2.4×10^{-1}
2-Methylphenanthrene	2.2×10^{-1}	(1.8×10^{-1})	1.5×10^{-1}	7.1×10^{-1}	(7.2×10^{-1})	2.7×10^{-1}
2-Methylanthracene	5.8×10^{-2}	(4.3×10^{-2})	8.6×10^{-2}	3.8×10^{-1}	(3.9×10^{-1})	1.5×10^{-1}
4- + 9-Methylphenanthrene [b]	1.3×10^{-1}	(1.1×10^{-1})	9.3×10^{-2}	5.3×10^{-1}	(5.9×10^{-1})	1.7×10^{-1}
1-Methylphenanthrene	2.1×10^{-1}	(1.8×10^{-1})	1.4×10^{-1}	7.4×10^{-1}	(7.8×10^{-1})	2.4×10^{-1}
4-Methylpyrene	1.2×10^{-1}	(1.2×10^{-1})	7.6×10^{-2}	6.4×10^{-1}	(5.6×10^{-1})	1.1×10^{-1}
1-Methylpyrene	1.3×10^{-1}	(1.3×10^{-1})	7.0×10^{-2}	5.8×10^{-1}	(5.0×10^{-1})	1.0×10^{-1}
1- + 3-Methylfluoranthene [b]	9.3×10^{-2}	(9.1×10^{-2})	5.7×10^{-2}	4.7×10^{-1}	(4.2×10^{-1})	9.9×10^{-2}
Methylfluoranthene + Methylpyrene [b, c]	7.4×10^{-2}	(7.3×10^{-2})	6.4×10^{-2}	6.0×10^{-1}	(4.8×10^{-1})	9.9×10^{-2}
Methylfluoranthene + Methylpyrene [b, c]	4.8×10^{-2}	(4.8×10^{-2})	3.5×10^{-2}	2.2×10^{-1}	(2.0×10^{-1})	5.0×10^{-2}
3-Methylchrysene	3.0×10^{-2}	(2.1×10^{-2})	1.7×10^{-2}	1.6×10^{-1}	(9.8×10^{-2})	5.8×10^{-2}
Methylchrysene + Methylbenz[a]anthracene [b, c]	1.1×10^{-2}	(1.1×10^{-2})	7.1×10^{-3}	6.1×10^{-2}	(3.3×10^{-2})	2.8×10^{-2}
Σ_{37}PAHs	9.9×10^{1}	(6.6×10^{1})	2.8×10^{1}	2.4×10^{2}	(1.1×10^{2})	1.5×10^{2}

[a] mean (standard deviation), n = 2.
[b] Not separated and quantified as a single compound.
[c] Not identified (native standard compounds not available).

Table 3. Average emission factors of OPAHs (mg kg^{-1}, dry mass basis) for both RWS (4* and 5*) in nominal and reduced output conditions. Measurements performed at the emission sampling location

Compounds	*4* RWS*			*5* RWS*		
	Nominal output		*Reduced output*	*Nominal output*		*Reduced output*
Phthaldialdehyde	3.3×10^{-3}	(2.3×10^{-3}) [a]	2.1×10^{-3}	5.4×10^{-3}	(2.6×10^{-3})	1.7×10^{-1}
1,4-Naphthoquinone	2.1×10^{0}	(1.9×10^{0})	1.4×10^{-1}	6.6×10^{-1}	(6.5×10^{-2})	4.1×10^{-1}
1-Naphthaldehyde	1.3×10^{1}	(7.7×10^{0})	1.5×10^{0}	2.0×10^{1}	(5.6×10^{0})	1.8×10^{0}
2-Formyl-trans-cinnamaldehyde	3.1×10^{-3}	(1.4×10^{-3})	3.6×10^{-3}	2.0×10^{-3}	(6.2×10^{-4})	5.7×10^{-3}
Benzophenone	4.4×10^{-2}	(1.9×10^{-2})	4.1×10^{-2}	5.2×10^{-2}	(3.5×10^{-2})	4.7×10^{-2}
1-Acenaphthenone	3.2×10^{0}	(1.0×10^{0})	7.7×10^{-1}	4.9×10^{0}	(1.5×10^{0})	2.4×10^{0}
9-Fluorenone	1.8×10^{0}	(1.4×10^{-2})	1.0×10^{0}	5.6×10^{-1}	(1.2×10^{-1})	1.2×10^{0}
Biphenyl-2-2′-dicarboxaldehyde	2.8×10^{-3}	(2.3×10^{-3})	1.6×10^{-3}	8.1×10^{-4}	(5.7×10^{-6})	8.6×10^{-4}
Xanthone	4.3×10^{-2}	(2.4×10^{-2})	2.0×10^{-2}	1.1×10^{-1}	(1.2×10^{-1})	2.1×10^{-1}
Acenaphthenequinone	1.8×10^{-2}	(1.8×10^{-2})	3.9×10^{-3}	8.7×10^{-3}	(2.3×10^{-3})	5.7×10^{-3}
Anthrone	1.5×10^{-2}	(8.6×10^{-3})	1.5×10^{-2}	2.7×10^{-2}	(2.0×10^{-2})	3.7×10^{-2}
6H-Dibenzo[b,d]pyran-6-one	1.3×10^{-1}	(1.3×10^{-1})	4.0×10^{-2}	2.3×10^{-1}	(1.6×10^{-1})	2.2×10^{-1}
9,10-Anthraquinone	4.1×10^{-1}	(4.0×10^{-1})	9.5×10^{-2}	7.3×10^{-1}	(5.1×10^{-1})	2.6×10^{-1}
1,8-Naphthalic anhydride	7.7×10^{-2}	(9.6×10^{-2})	9.1×10^{-3}	4.2×10^{-2}	(2.2×10^{-2})	3.8×10^{-1}
1,4-Anthraquinone	1.7×10^{-3}	(2.4×10^{-3})	4.7×10^{-3}	1.9×10^{-3}	(1.2×10^{-3})	5.2×10^{-2}
4,4′-Biphenyldicarboxaldehyde	3.9×10^{-3}	(3.5×10^{-3})	4.1×10^{-3}	9.0×10^{-4}	(3.5×10^{-4})	1.7×10^{-3}
2-Methylanthraquinone	2.2×10^{-2}	(1.9×10^{-2})	1.6×10^{-2}	6.9×10^{-3}	(6.3×10^{-3})	3.6×10^{-2}
9-Phenanthrene carboxaldehyde	2.6×10^{-2}	(2.1×10^{-2})	6.1×10^{-3}	2.8×10^{-2}	(8.9×10^{-3})	1.2×10^{-2}
9,10-Phenanthrenequinone	1.1×10^{-2}	(9.0×10^{-3})	3.0×10^{-3}	9.0×10^{-3}	(1.8×10^{-3})	1.5×10^{-3}
2-Nitro-9-fluorenone	2.7×10^{-3}	(1.4×10^{-3})	1.0×10^{-3}	5.4×10^{-4}	(1.6×10^{-4})	6.2×10^{-4}
Benzo[a]fluorenone	1.3×10^{-1}	(1.2×10^{-1})	3.7×10^{-2}	3.4×10^{-1}	(5.8×10^{-2})	9.8×10^{-2}
Benzo[b]fluorenone	2.0×10^{-1}	(1.9×10^{-1})	3.7×10^{-2}	5.6×10^{-1}	(1.4×10^{-1})	3.4×10^{-1}
Benzanthrone	7.0×10^{-1}	(6.9×10^{-1})	1.2×10^{-1}	4.9×10^{0}	(2.1×10^{0})	3.3×10^{0}
1-Pyrene carboxaldehyde	3.3×10^{-2}	(3.0×10^{-2})	7.9×10^{-3}	9.2×10^{-2}	(1.8×10^{-2})	6.5×10^{-2}
Aceanthrenequinone	2.8×10^{-2}	(2.3×10^{-2})	5.1×10^{-3}	1.3×10^{-1}	(1.3×10^{-1})	1.9×10^{-2}
Benz[a]anthracene-7,12-dione	7.8×10^{-2}	(6.6×10^{-2})	1.4×10^{-2}	1.1×10^{-1}	(6.9×10^{-3})	7.6×10^{-2}
1,4-Chrysenequinone	6.1×10^{-3}	(2.9×10^{-3})	2.0×10^{-3}	2.4×10^{-3}	(1.6×10^{-4})	1.0×10^{-2}
Σ_{27}OPAHs	2.2×10^{1}	1.3×10^{1}	3.9×10^{0}	3.3×10^{1}	7.2×10^{0}	1.1×10^{1}

[a] mean (standard deviation), n = 2.

Table 4. Average emission factors of NPAHs (mg kg^{-1}, dry mass basis) for both RWS (4* and 5*) in nominal and reduced output conditions. Measurements performed at the emission sampling location

Compounds	*4* RWS*			*5* RWS*		
	Nominal output		*Reduced output*	*Nominal output*		*Reduced output*
1-Nitronaphthalene	1.8×10^{-2}	(1.2×10^{-2}) [a]	4.6×10^{-3}	5.8×10^{-3}	(1.1×10^{-3})	5.6×10^{-3}
2-Methyl-1-NN+1-Methyl-5-NN	3.7×10^{-3}	(1.7×10^{-3})	3.7×10^{-3}	8.4×10^{-4}	(2.6×10^{-5})	3.9×10^{-3}
2-Nitronaphthalene	1.7×10^{-2}	(1.4×10^{-2})	4.9×10^{-3}	6.2×10^{-3}	(9.9×10^{-4})	5.3×10^{-3}
2-Methyl-4-nitronaphthalene	1.7×10^{-3}	(1.1×10^{-3})	8.2×10^{-4}	5.5×10^{-4}	(3.4×10^{-5})	7.9×10^{-5}
1-Methyl-4-nitronaphthalene	7.5×10^{-4}	(4.8×10^{-4})	5.6×10^{-4}	6.9×10^{-4}	(8.5×10^{-6})	1.1×10^{-3}
1-Methyl-6-nitronaphthalene	1.0×10^{-3}	(8.4×10^{-4})	1.0×10^{-3}	1.3×10^{-4}	(1.8×10^{-4})	4.2×10^{-4}
1,5-Dinitronaphthalene	8.3×10^{-4}	(6.8×10^{-4})	0.0×10^{0}	2.3×10^{-4}	(7.0×10^{-5})	4.4×10^{-4}
2-Nitrobiphenyl	2.5×10^{-3}	(1.8×10^{-3})	1.1×10^{-3}	7.3×10^{-4}	(1.2×10^{-4})	4.7×10^{-4}
3-Nitrobiphenyl	2.0×10^{-3}	(1.2×10^{-3})	1.3×10^{-3}	6.4×10^{-4}	(9.9×10^{-5})	7.1×10^{-3}
3-Nitrodibenzofuran	2.8×10^{-3}	(2.7×10^{-3})	5.6×10^{-4}	1.1×10^{-3}	(2.3×10^{-4})	2.8×10^{-3}
5-Nitroacenaphthene	4.4×10^{-4}	(3.6×10^{-4})	1.8×10^{-4}	2.5×10^{-4}	(3.6×10^{-4})	5.6×10^{-4}
2-Nitrofluorene	0.0×10^{0}	(0.0×10^{0})	0.0×10^{0}	1.9×10^{-4}	(5.0×10^{-5})	0.0×10^{0}
9-Nitroanthracene	7.6×10^{-4}	(6.9×10^{-4})	3.9×10^{-4}	4.7×10^{-4}	(1.9×10^{-4})	1.0×10^{-2}
9-Nitrophenanthrene	1.1×10^{-3}	(9.3×10^{-4})	4.9×10^{-4}	3.2×10^{-4}	(7.9×10^{-5})	0.0×10^{0}
2-Nitrodibenzothiophene	1.2×10^{-3}	(1.7×10^{-3})	5.7×10^{-4}	3.3×10^{-3}	(7.3×10^{-5})	6.0×10^{-4}
3-Nitrophenanthrene	1.4×10^{-3}	(1.2×10^{-3})	6.0×10^{-4}	3.9×10^{-4}	(6.5×10^{-5})	5.7×10^{-4}
2-Nitroanthracene	8.2×10^{-4}	(6.4×10^{-4})	6.2×10^{-4}	7.2×10^{-4}	(2.3×10^{-4})	0.0×10^{0}
2-Nitrofluoranthene	2.4×10^{-3}	(2.2×10^{-3})	9.7×10^{-4}	9.3×10^{-4}	(2.4×10^{-4})	1.0×10^{-3}
3-Nitrofluoranthene	2.6×10^{-3}	(2.3×10^{-3})	1.2×10^{-3}	9.4×10^{-4}	(1.2×10^{-4})	3.4×10^{-4}
4-Nitropyrene	5.3×10^{-3}	(4.1×10^{-3})	1.5×10^{-3}	4.7×10^{-3}	(8.8×10^{-4})	3.1×10^{-3}
1-Nitropyrene	1.9×10^{-3}	(1.7×10^{-3})	8.8×10^{-4}	6.1×10^{-4}	(2.2×10^{-5})	4.1×10^{-3}
2-Nitropyrene	4.1×10^{-4}	(5.7×10^{-4})	1.1×10^{-3}	9.2×10^{-3}	(1.1×10^{-2})	2.3×10^{-3}
7-Nitrobenz[a]anthracene	0.0×10^{0}	(0.0×10^{0})	0.0×10^{0}	6.1×10^{-4}	(1.4×10^{-4})	0.0×10^{0}
6-Nitrochrysene	1.9×10^{-3}	(1.6×10^{-3})	1.0×10^{-3}	3.8×10^{-4}	(8.3×10^{-5})	7.8×10^{-5}
1,3-Dinitropyrene	7.4×10^{-4}	(1.0×10^{-3})	0.0×10^{0}	3.0×10^{-3}	(6.2×10^{-5})	5.9×10^{-4}
1,6-Dinitropyrene	0.0×10^{0}	(0.0×10^{0})	0.0×10^{0}	0.0×10^{0}	(0.0×10^{0})	0.0×10^{0}
1,8-Dinitropyrene	0.0×10^{0}	(0.0×10^{0})	2.8×10^{-3}	2.3×10^{-2}	(2.9×10^{-2})	4.5×10^{-4}
1-Nitrobenzo[e]pyrene	7.8×10^{-4}	(1.1×10^{-3})	0.0×10^{0}	2.7×10^{-3}	(2.0×10^{-3})	3.9×10^{-4}
6-Nitrobenzo[a]pyrene	6.0×10^{-3}	(4.6×10^{-3})	0.0×10^{0}	5.7×10^{-3}	(6.5×10^{-3})	0.0×10^{0}
3-Nitrobenzo[e]pyrene	0.0×10^{0}	(0.0×10^{0})	0.0×10^{0}	6.6×10^{-4}	(5.1×10^{-4})	0.0×10^{0}
Σ_{31}NPAHs	7.8×10^{-2}	(5.8×10^{-2})	3.1×10^{-2}	7.5×10^{-2}	(4.7×10^{-2})	5.1×10^{-2}

[a] mean (standard deviation), n = 2.

Figures

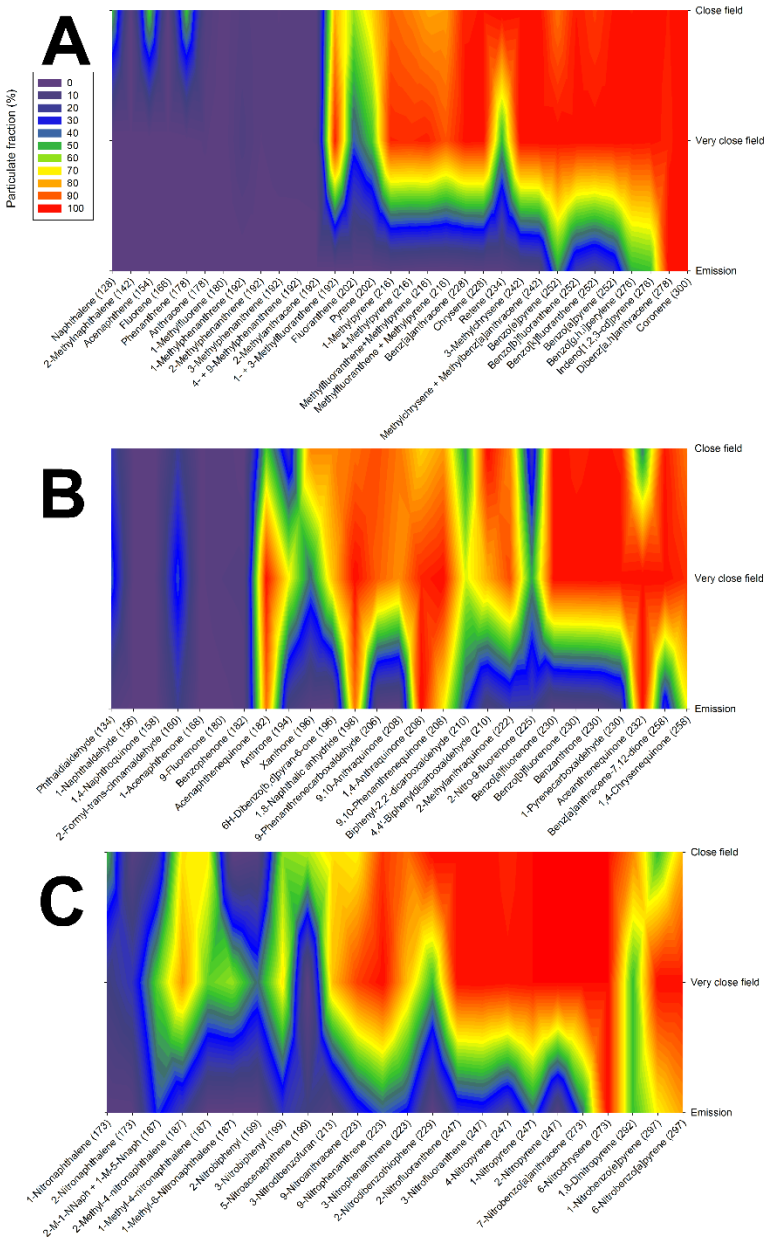

Figure 1. PAH (A), OPAH (B) and NPAH (C) gas/particle partitioning evolution from emission until close field according to their molecular weight (5* RWS, nominal output). Results in VCF from the heated emission sampling train measurement method. Note, in this graphical representation, that there is no link between the compounds on the X-axis.

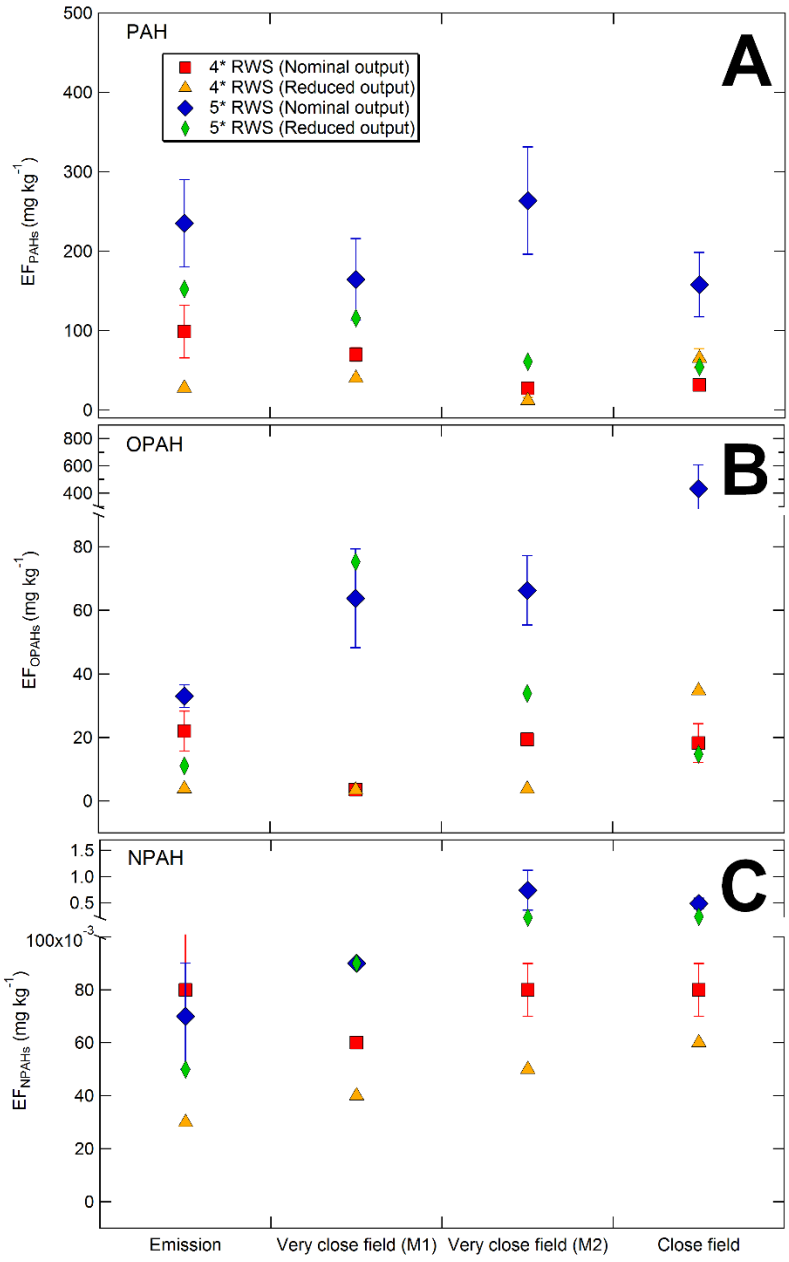

Figure 2. Comparison of the equivalent emission factor of PAHs (EF Σ_{37}PAHs) (A), OPAHs (EF Σ_{27}OPAHs) (B)and NPAHs (EF Σ_{31}NPAHs) (C) (mg kg^{-1}) from emission until close field for both RWS and combustions conditions (nominal and reduced outputs). The error bars correspond to the standard deviation for the duplicate experiments in nominal output conditions. Note that the Y-axis is split.

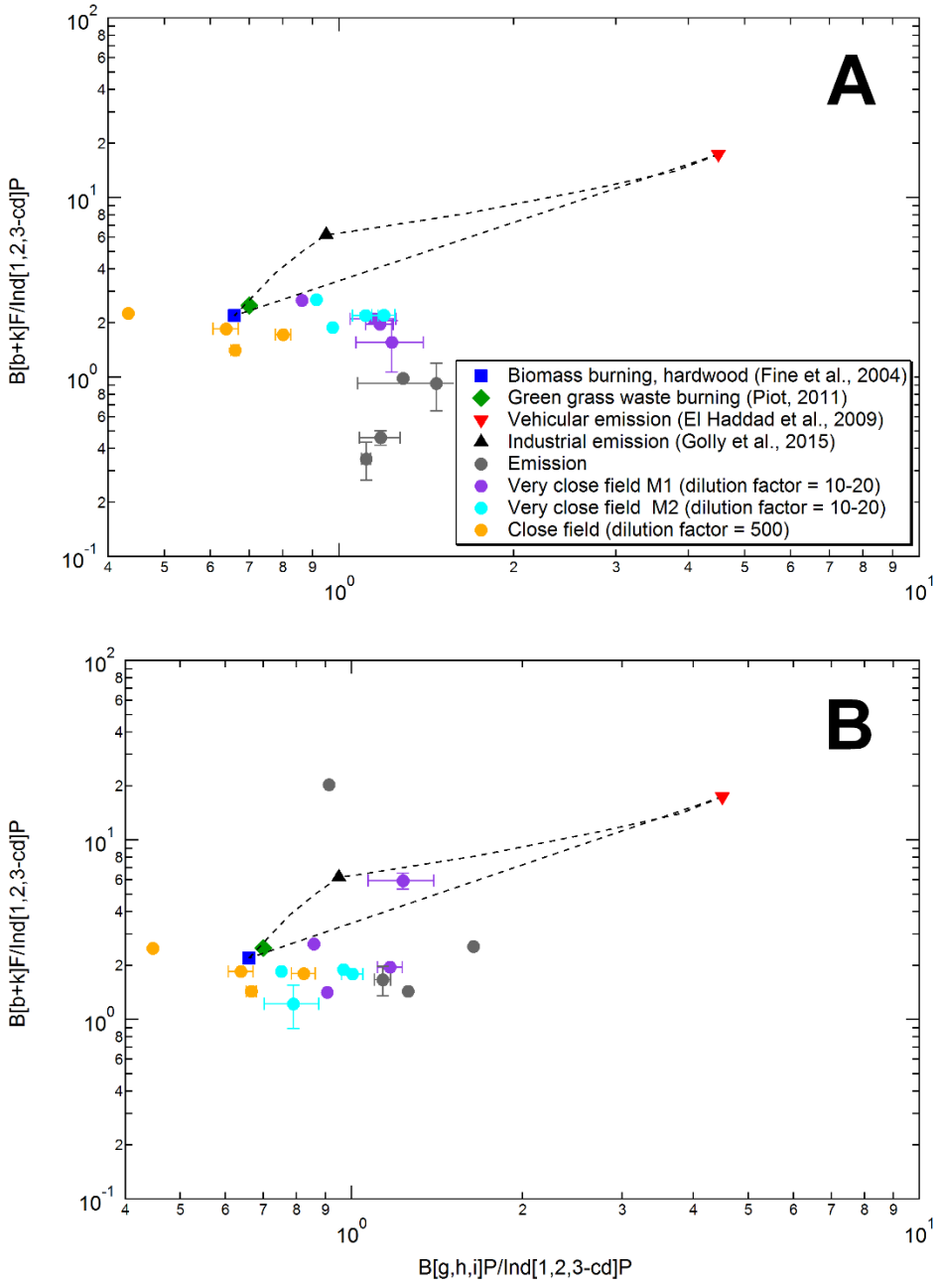

Figure 3. Ratio-ratio plot for the evaluation of PAH sources. Application to the results taking into account the particulate phase only (A) and both, gaseous and particulate phases (B). M1 and M2: two measurement methods carried out in parallel in VCF, heated emission sampling train and Partisol sampler, respectively. The error bars show the standard deviations for the duplicate experiments.

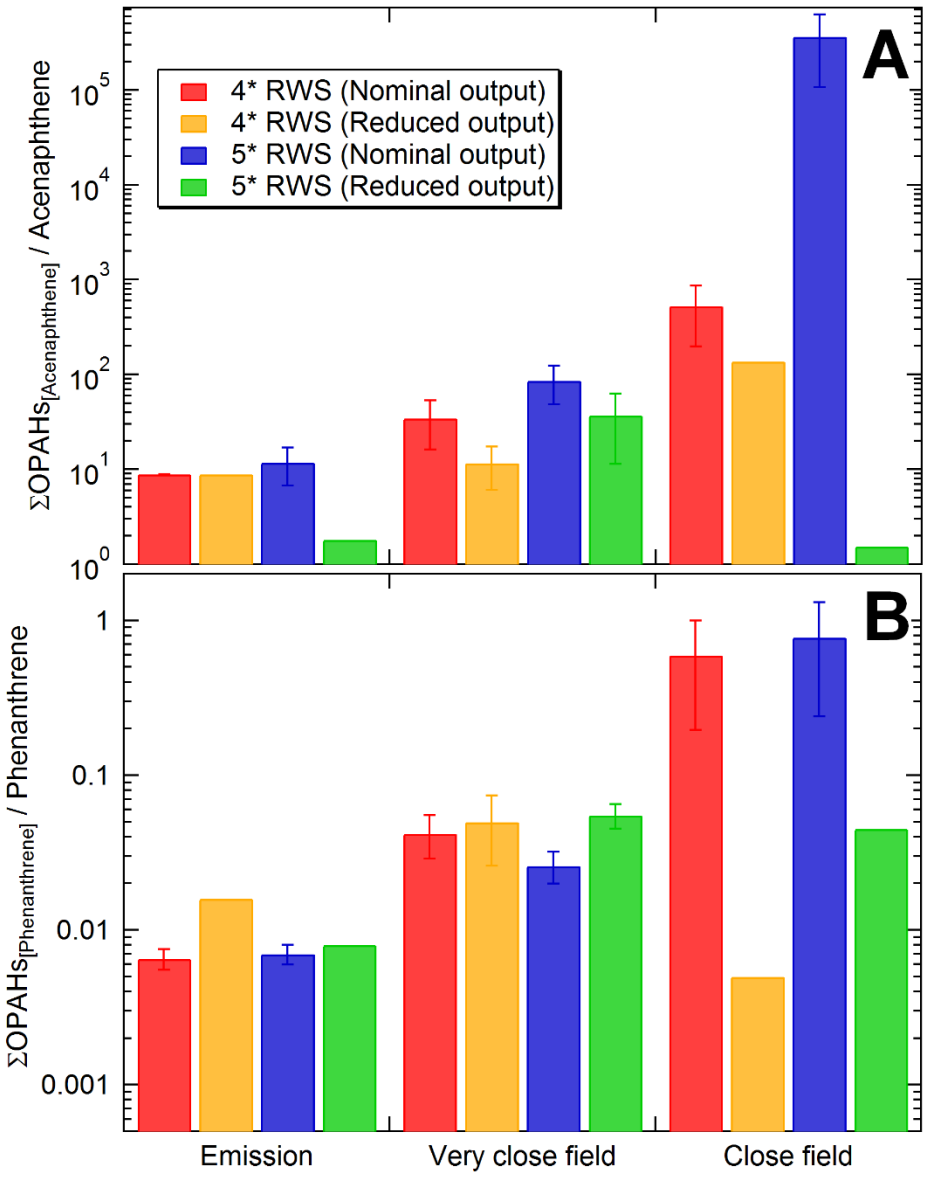

Figure 4. Evolution from emission until close field of the ratio of the sum of Acenaphthene OPAH derivatives/ Acenaphthene ($\Sigma OPAHs_{[Acenaphthene]}$/ Acenaphthene) (A) and Phenanthrene OPAH derivatives/Phenanthrene ($\Sigma OPAHs_{[Phenanthrene]}$/Phenanthrene) (B) (gaseous + particulate phases). The error bars correspond to the standard deviation for the duplicate experiments in nominal output condition, and for both measurement methods (M1 and M2) used in VCF. Y-axis is in log scale.

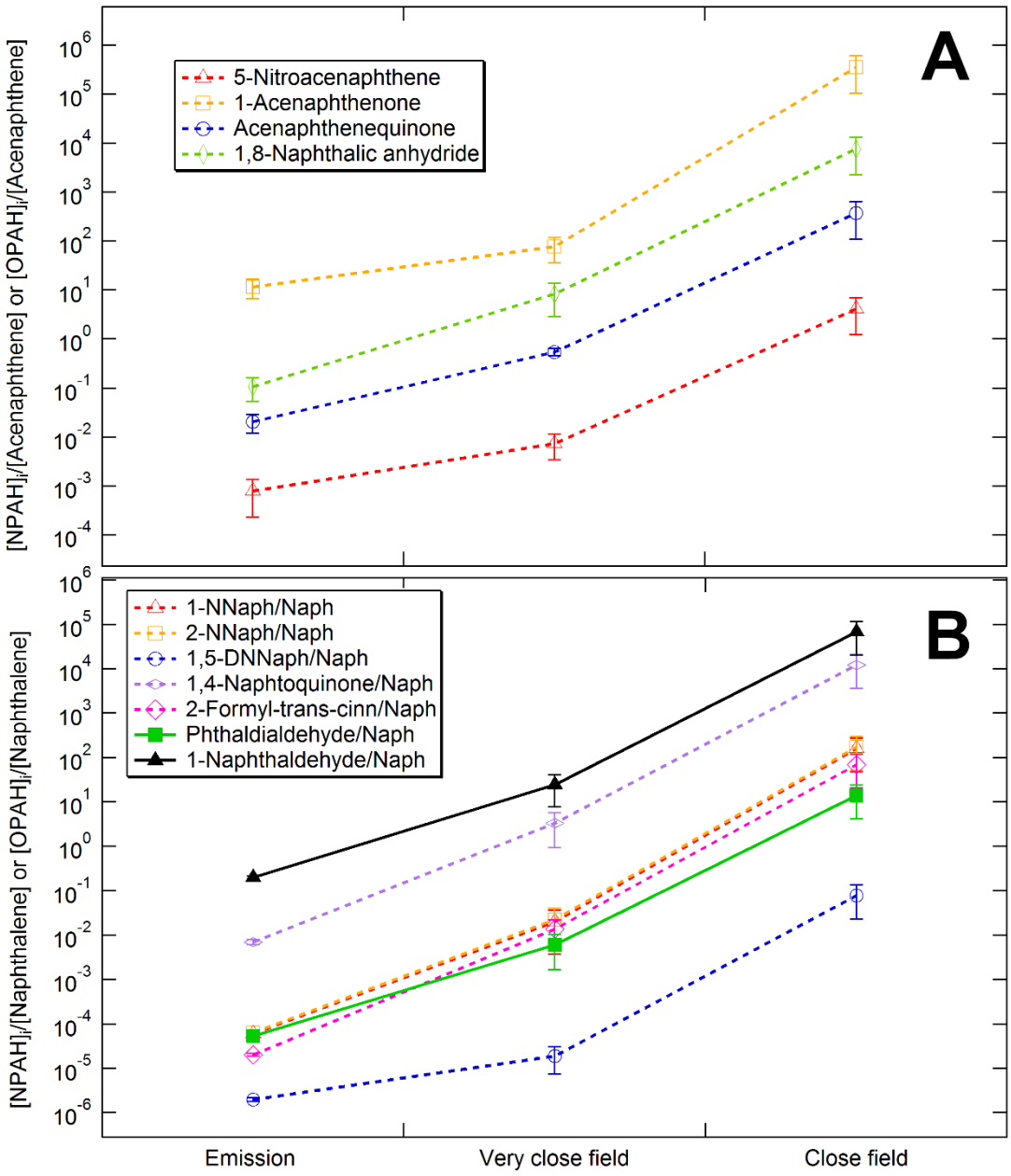

Figure 5. Evolution from emission until close field of the individual ratios of Acenaphthene OPAH or NPAH derivatives/Acenaphthene (A) and Naphthalene OPAH or NPAH derivatives/Naphthalene (B) for the 5* RWS in nominal output conditions. The error bars correspond to the standard deviation for the duplicate experiments in nominal output conditions and for both measurement methods (M1 and M2) used in VCF. Y-axis is in log scale.